Adaptive Patch Projection for the Generation of Orthophotos from Satellite Images

Liang-Chien Chen, Tee-Ann Teo, and Jiann-Yeou Rau

Abstract

In this paper, we describe an "Adaptive Patch Projection" scheme that can accelerate the orthorectification for satellite images without losing accuracy. The proposed scheme is comprised of two major components: (a) orbit modeling, and (b) image orthorectification. In orbit modeling, we provide a collocation procedure to determine the precise orbits. In image orthorectification, the area of interest is sequentially subdivided into four quadrate tiles until a specified threshold for terrain variations is met. The threshold of maximum terrain variation in a tile will be optimized according to the computational efficiency and the accuracy requirements. Once the ground tiles are determined, we perform adaptive patch projection to the corresponding image pixels. Test images from SPOT5 Supermode and QuickBird satellites are included. The experimental results show that this algorithm can minimize the orthorectification computation time, while the modeling error is insignificant.

Introduction

The most rigorous way to register a remotely sensed image with a relevant spatial data layer is to perform orthorectification on the image. The generation of orthophoto images from remote sensing images is an important task for various remote sensing applications, such as cartography, environmental monitoring, and city planning. Moreover, GIS technology often needs multi-temporal images for the detection of land-cover changes. Thus, ortho-rectified images have become important, primarily due to their short production time.

Currently, most high-resolution satellites such as SPOT5, Ikonos, QuickBird, and others use linear pushbroom arrays. A number of investigations regarding the geometric accuracy for these pushbroom linear array images have been made (Westin, 1990; Chen and Lee, 1993; Orun and Natarajan, 1994; Toutin, 2003). Traditionally, the first step in image orthorectification is to model the orientation parameters by using ground control points. Then, by incorporating a DTM, an image, and the orientation parameters, a non-linear equation is formulated to determine the along-track image coordinates for a ground element in terms of the sampling time. The across-track image coordinates can thus be calculated according to the collinearity condition equations.

The traditional solutions for the orthorectification of pushbroom images are time-consuming due to a vast number of non-linear equations that have to be solved. This weakness is so obvious that for high-resolution satellite images, a more efficient way to reach a solution is required. Konecny *et al.* (1987) considered SPOT images as center perspective, then, implemented the idea on an analytical plotter, to achieve real time operation, while maintaining some accuracy. Inspired by this idea, we propose an "Adaptive Patch Projection" procedure for accelerating the orthorectification computations for high-resolution satellite images with large number of pixels.

For the small field-of-view (FOV) of a high-resolution satellite, the relief displacements in a small area with moderate terrain variations may be assumed to be linear. We can, thus, propose a method that can do the orthorectification patch-by-patch. The patch size may be adapted to suit different terrain characteristics. We first divide the area of interest into a number of tiles. For the corner point with the highest elevation, we compute the image coordinate for each corner point of the tile using an indirect, i.e., bottom-up method. The indirect method is also applied to the corner point with the lowest elevation. An affine transformation is used as a mapping function for image coordinates and object coordinates. In addition, we need to analyze terrain variations in order to select the adaptive window of the tiles. We also analyze the modeling error for the proposed method, including the transformation error and the interpolation error. Affine transformation, the patch size, tilt angle, and elevation range are the most important factors that need to be considered.

The structure of this paper is as follows. We discuss the techniques behind the proposed scheme, then, analyze the modeling error of the proposed scheme. We apply the proposed scheme to two real cases, including SPOT5 and QuickBird images, followed by some conclusions.

The Proposed Scheme

The proposed method is comprised of two major parts. In the first part, the satellite orientation is modeled by employing ground control points. In the second part, the orbital parameters are utilized to perform the orthorectification, using the proposed "Adaptive Patch Projection" method. The modeling error of the "Adaptive Patch Projection" model will also be evaluated in this section.

Orbit Adjustment

In the modeling of the orientation parameters, the position vectors and the attitudes of the satellite are expressed with low order polynomials in terms of sampling time. Due to the

Center for Space and Remote Sensing Research, National Central University, Chung-Li, Taiwan (lcchen@csrsr.ncu.edu.tw).

Photogrammetric Engineering & Remote Sensing
Vol. 71, No. 11, November 2005, pp. 1321–1327.

0099-1112/05/7111–1321/$3.00/0

extremely high correlation between the two groups of orbital parameters and the attitude data, we only adjust the orbital parameters, followed by a collocation procedure to compensate for the local systematic errors. Two steps are included in the orientation modeling. In the first step, the orientation parameters are initialized using on-board ephemeris data. We then fit the orbital parameters with low order polynomials using GCPs. Once the trend functions of the orbital parameters are determined, the fine-tuning of an orbit is performed using the least squares filtering (also called the "least squares collocation") technique (Mikhail and Ackermann, 1982).

Preliminary Orbit Fitting

On-board data include a certain degree of errors; therefore, GCPs are needed to adjust the orbital parameters. The observation vector will not pass through the corresponding GCPs due to errors in the on-board data (Chen and Chang, 1998; Chen and Teo, 2001). Thus, correction of the orbital data may be performed under collinearity conditions.

Least Squares Filtering

Due to the fact that the above least squares fitting procedure is a global treatment method, it cannot compensate for local systematic errors. Therefore, least squares filtering has to be used to fine tune the orbit. By doing this, we assume that the *x*, *y*, and *z* axes are independent, using three one dimension functions to adjust the orbit. The least squares filtering model is shown as follows:

$$\rho_k = \overrightarrow{c_k}[C_k]^{-1}\overrightarrow{\varepsilon_k} \quad \text{k} = x,y,z \text{ axis}, \tag{1}$$

where ρ_k = correction value of the intersection point after least squares filtering; c_k = covariance matrix of the intersection point with respect to each GCP; C_k = covariance matrix for each pair of GCPs; and ε_k = residuals of the GCPs.

The number of GCPs is, in general, insufficient to characterize the covariance function. We, thus, select a Gaussian function with some empirical values for the covariance function, as shown in Equation 2:

$$\textit{Covariance} = \begin{Bmatrix} (1 - r_n)\mu_k e^{-\left(2.146\frac{d}{d_{\max}}\right)^2}, & \textit{if} \quad d \neq 0 \\ \mu_k, & \textit{if} \quad d = 0 \end{Bmatrix} \tag{2}$$

where d = distance between an intersection point and a GCP; $d_{\max}$ = maximum distance to the intersection point; μ_k = variance of the GCP residual; and r_n = filtering ratio (in the experiment we use 0.2).

This empirical value, 2.146, is selected so that the covariance limit is $1\% \times (1 - r_n)\ \mu_k$, when $d = d_{\max}$.

Orthorectification

The essential task in image orthorectification is to determine the image pixel corresponding to a ground element. In addition to providing the traditional pixel-by-pixel procedure, we outline the proposed patch projection method. An adaptive patch approach that considers terrain variations is also discussed.

It has been demonstrated that the indirect method performs better than the direct method in terms of quality and efficiency (Kim *et al.*, 2001). Thus, we select the indirect method to determine the image pixel corresponding to a ground element.

Figure 1 shows the geometry for the indirect method. Given a ground point **A**, we can create a vector **r(t)**, from ground point **A** to image point **a**. The vector **r(t)** vector is located on the principle plane and **n(t)** is the normal vector on the principal plane. The mathematics show that, at time *t*, **r(t)** is orthogonal to the normal vector **n(t)**. When **r(t)** is perpendicular to **n(t)**, the inner product of **r(t)** and **n(t)** is zero. Function **f(t)** is defined as characterizing the coplanarity condition:

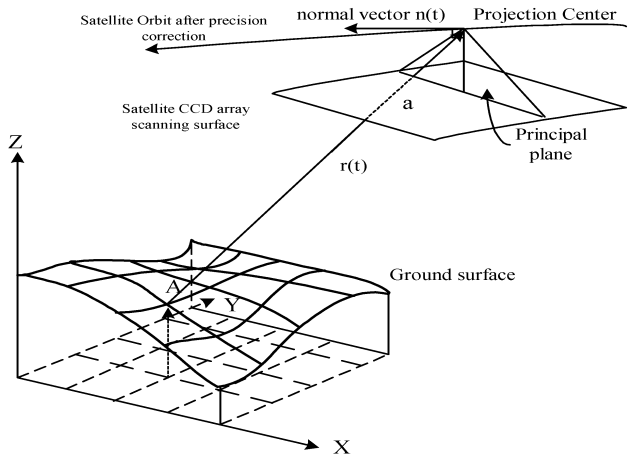

Figure 1. Illustration of the indirect method.

$$\mathbf{f(t)} = \mathbf{r(t)} \cdot \mathbf{n(t)} = 0 \tag{3}$$

We apply Newton-Raphson method to solve the nonlinear Equation 3 and to determine the sampling time *t*, for ground point **A**.

For an image point sampled at time *t*, we can decide on the principal plane; the along track image coordinates can be calculated with Equation 4:

$$\text{Line} = (t - t_0)/(\text{Integration Time}) \tag{4}$$

where t = sampling time; t_0 = sampling time for first scan line; and Integration Time = sampling interval.

The across track image coordinates may now be determined. In the principal plane, the FOV is determined by the pointing vectors of the first CCD and the last one. The angle *S* between the pointing vector of the first CCD and observation vector **r(t)** can be calculated. The across track coordinates can be calculated by using Equation 5:

$$\text{Sample} = (S/\text{FOV})^*\text{PixelsPerLine} \tag{5}$$

where S = angle between the vector of the first CCD and **r(t)**; FOV = field of view angle; and PixelsPerLine = number of pixels in a line.

Patch Projection

The indirect pixel-by-pixel method is very time consuming. Thus, we propose a "Patch Projection" method which minimizes the orthorectification computation load but preserves a negligible model error. The proposed method is based on the following two assumptions: (a) the relief displacements in a small area with moderate terrain variations are linear; and (b) the mapping geometry between the images coordinates, and the object coordinates may be expressed by an affine transformation, when a small area is considered.

The procedure of the patch projection is illustrated in Figure 2. We first divide the area of interest into a number of equal-sized tiles. We select the lowest elevation in the tile, and the corners of the tile are projected on the image to form a set of anchor points. Another set of anchor points for the highest elevation are generated in the same manner. If we assume that the relief displacement in a small tile is

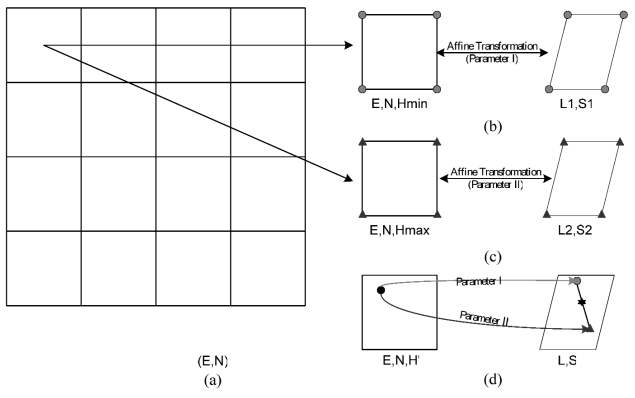

Figure 2. Illustration of patch projection. (a) equal sized tiles, (b) anchor point generation for the top layer, (c) anchor point generation for the bottom layer, (d) interpolation.

linear, a groundel within the tile can be projected into the image space according to the groundel elevation and the two associated anchor point sets.

Adaptive Patch Projection

To reduce the interpolation error when terrain variation is considered, it is better that the patch size changes according to the terrain characteristics. The patch size should be large for rolling terrain and small for rugged terrain. The quadtree structure (Mather, 1999), which segments the terrain coverage for a given elevation range, is a straightforward and yet effective way to characterize terrain variations. Based on this performance, we selected the quadtree structure to help adapt the window size in the patch projection procedure.

The method discussed in this section is a modification of the one discussed in the previous section. In the quadtree analysis, the allowed elevation range is selected so that the model error will not exceed the tolerance. An analysis of the model error will be discussed in the next section. After subdividing the terrain, tiles with different sizes are projected into the image space one by one using the process described in the previous section.

Analysis of Modeling Errors

Two steps, affine transformation for anchor point sets and linear interpolation, may introduce modeling errors into the patch projection. In the imaging geometry, the patch size, tilt angle, and elevation range are the three most important factors that need to be considered in the analysis of modeling errors. Simulations based on SPOT5 Supermode images and QuickBird Panchromatic images are employed; both include the largest number of pixels among the high-resolution satellite imagery for this demonstration. The modeling error is defined as the difference between the proposed method and a rigorous point-by-point backprojection.

Error Simulation for SPOT5 Supermode Images

The evaluation items and parameters are shown in Table 1; the tilt angle is less than 30°. The elevation ranges from 0 m to 2,000 m. The patch size is within 40 m by 40 m and 3,000 m by 3,000 m.

Affine Transformation Modeling Error: Given a tilt angle of 30° and elevations of 0 m and 2,000 m, the errors due to affine transformation are shown in Figure 3. In this investigation, we can see that when a patch size of 1,500 m by 1,500 m is selected, the modeling error falls within the tolerance level, i.e., 0.05 pixels.

Terrain Variation Modeling Error: Given a tilt angle of 30°, the errors due to terrain variation are shown in Figure 4. In this investigation, when the terrain variation is less than 1,000 m and the patch size is less than 640 m by 640 m, the modeling error falls within the tolerance level, i.e., 0.05 pixels.

Tilt Angle Modeling Error: Figure 5 shows the errors due to the tilt angle when the terrain variation is less than 1,000 m. The results indicate that when the patch size is smaller than 640 m by 640 m, the modeling error is smaller than 0.05 pixels for the different tilt angles.

Error Simulation for QuickBird Panchromatic Images

The evaluation items and parameters are shown in Table 2. The tilt angle is less than 30°, and the elevation ranges from 0 m to 1,000 m. Because the QuickBird panchromatic resolution is a quarter that of SPOT5 supermode resolution, the QuickBird patch size is quarter that of the SPOT5 patch size, the patch size is within 8 m by 8 m and 500 m by 500 m.

Affine Transformation Modeling Error: Figure 6 shows the errors due to affine transformation given a tilt angle of 30° and elevation at 0 m to 1,000 m. In this investigation, it is indicated that when a patch size of 500 m by 500 m is selected, the modeling error is within the tolerance level, i.e., 0.05 pixels.

Terrain Variation Modeling Error: Figure 7 shows the errors due to terrain variation given a tilt angle of 30°. In this investigation, it is indicated that when the terrain variation is less than 350 m and patch size less than 160 m by 160 m, the modeling error is within the tolerance level, i.e., 0.05 pixels.

Tilt Angle Modeling Error: Figure 8 shows the errors due to the tilt angle given a terrain variation of 350 m. It is indicated that when the patch size is smaller than 160 m by 160 m, the modeling error is smaller than 0.05 pixels for different tilt angles.

TABLE 1. SPOT5 MODELING ERROR ANALYSIS

Evaluation Item / Variable	Transformation Model Error	Interpolation Model Error	
	Affine Transformation	Variation of Terrain	Tilt Angle
Tilt Angle (degrees)	30	30	1 to 30*
Elevation (meters)	0 and 2000	0 to 2000**	0 and 1000
Patch Size (meters × meters)	40 × 40 to 3000 × 3000***	40 × 40 to 3000 × 3000***	40 × 40 to 3000 × 3000***

*Tilt angle step (degrees): 1, 2, 4, 8, 16, 20, 25, and 30.
**Elevation step (meters): 5, 10, 20, 40, 80, 160, 320, 500, 640, 750, 1000, and 2000.
***Patch size step (meters): 40, 80, 160, 320, 640, 1280, 1500, 2000, 2500, and 3000.

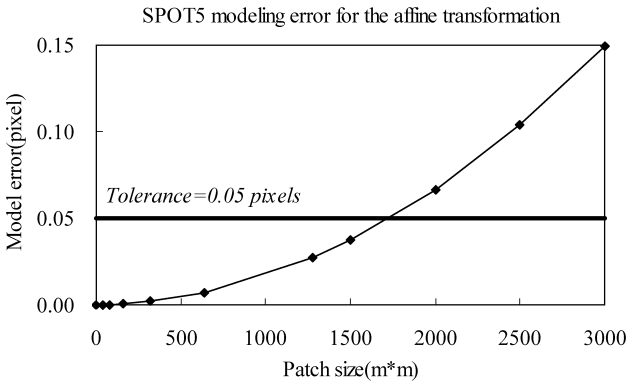

Figure 3. SPOT5 modeling error for the affine transformation.

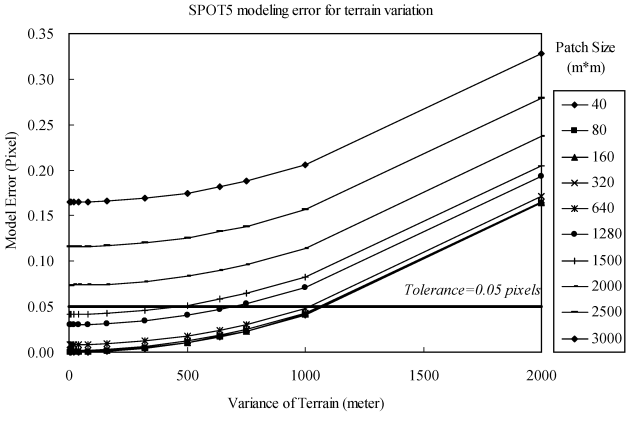

Figure 4. SPOT5 modeling error for terrain variation.

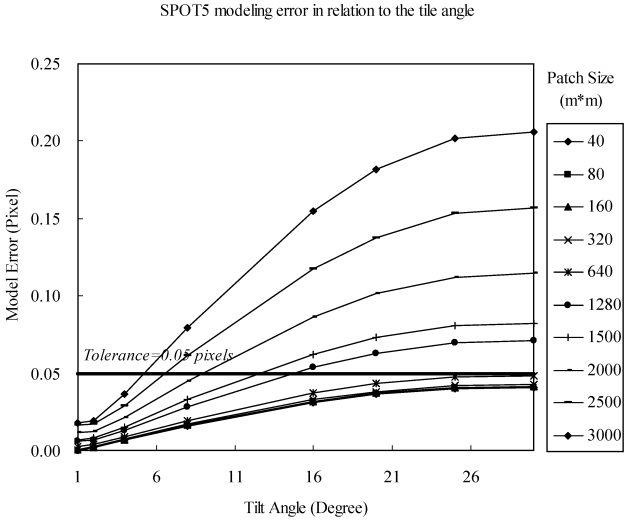

Figure 5. SPOT5 modeling error in relation to the tilt angle.

Experimental Results

The test data include SPOT5 and QuickBird images. The ground control points (GCPs) and independent check points (ICPs) are measured from 1:1000 scale topographic maps. The position accuracy is better than 50 centimeters. The number of points are 49 and 23 for SPOT5 and QuickBird cases, respectively. The elevation ranges for the SPOT5 and QuickBird images are 0 m to 2,100 m and 0 m to 700 m, respectively. The related information is shown in Table 3.

The experiment includes three parts: (a) patch size selection for test data, (b) accuracy analysis, and (c) computation time analysis. In order to get the adaptive patch size, we set a model error tolerance for the analysis; the real ephemeris data and simulated terrain are considered in the analysis. When the patch size is determined, we check the accuracy of the orbit modeling and examine the accuracy of the generated orthophoto image. The difference between the orbit modeling and the orthophoto image corresponds to the modeling error. The computation time for equal patch projection and adaptive patch projection is also compared in point-by-point.

Patch Size Selection

The differences in the covered area and the elevation ranges, between the SPOT5 and QuickBird images are 40 m to 2,000 m and 40 m to 600 m, respectively. Given tilt angles of 14.23° and 12.52° for the two satellites, the modeling errors behave as shown in Figure 9. It is expected that a larger patch size will lead to less computation time. In these two test cases the modeling error tolerance is selected to be 0.05 pixels. Thus, the patch for both sensors should be 160 m by 160 m and the terrain variation should be smaller than 500 m.

Accuracy Analysis

The ray-tracing method is applied to evaluate the orbit accuracy. Given the satellite orientation and the image points, we can calculate the intersection point of the DTM and the ray direction. Table 4 illustrates the accuracy performance of GCPs and ICPs, when nine GCPs are employed. We can see that the accuracy of SPOT5 and QuickBird was better than two pixels in orbit modeling.

In order to evaluate the quality of an orthophoto image, we must check it by a sufficient number of checkpoints. Table 4 shows the orthorectification RMSE. It is observed that the RMSE behaves similar to the orbit modeling. The error vectors for SPOT5 are illustrated in Figure 10, and the error vectors for QuickBird are illustrated in Figure 11. In Figures 10 and 11, triangles represent the GCPs, while the circles represent the ICPs. Note that the accuracy results for the orthoimages are similar to the ones for orbit modeling which indicates that loss of accuracy is insignificant.

Computation Time

We used a personal computer with a 3GHZ CPU for the orthorectification process; the equal grid patch projection method was applied in the orthorectification. We set up that the model error should be less than 0.05 pixels in patch projection. Referring to Table 3, for the SPOT5 and QuickBird data, the variance of the terrain in a single tile should be smaller than 500 m. We used the actual DTM to do the terrain analysis for both sensors. The elevation range of SPOT5 is from 0 m to 2,100 m, when the terrain variation is smaller than 500 m in a single tile. A smaller patch size is 160 m by 160 m, so we use a 160 m by 160 m sized tile to do the equal grid patch projection. The elevation range of QuickBird is between 50 m to 700 m. We analyze the DTM with respect to QuickBird, when the terrain variation is smaller than 500 m in a single tile; the smaller patch size is

TABLE 2. QUICKBIRD MODELING ERROR ANALYSIS

Variable \ Evaluation Item	Transformation Model Error	Interpolation Model Error	
	Affine Transformation	Variation of Terrain	Tilt Angle
Tilt Angle (degrees)	30	30	1 to 30*
Elevation (meters)	0 and 1000	0 to 1000**	0 and 350
Patch Size (meter × meter)	8 × 8 to 500 × 500***	8 × 8 to 500 × 500***	8 × 8 to 500 × 500***

*Tilt angle step (degrees): 1, 2, 4, 8, 16, 20, 25, and 30.
**Elevation step (meters): 5, 10, 20, 40, 80, 160, 320, 500, 640, 750, and 1000.
***Patch size step (meters): 8, 16, 32, 64, 128, 160, 256, 300, 400, and 500.

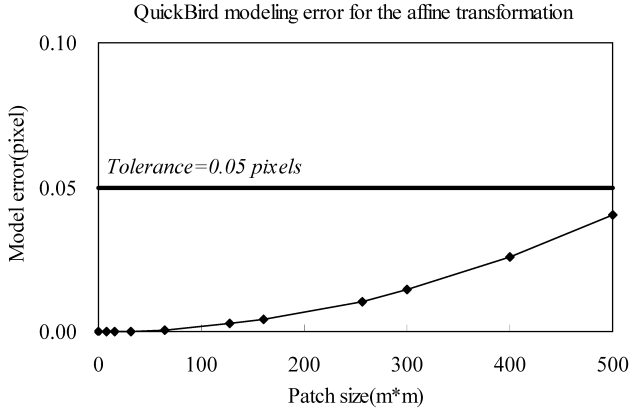

Figure 6. QuickBird modeling error for the affine transformation.

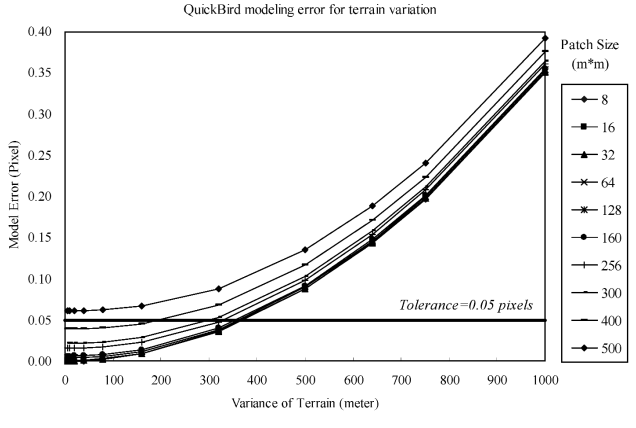

Figure 7. QuickBird modeling error for terrain variation.

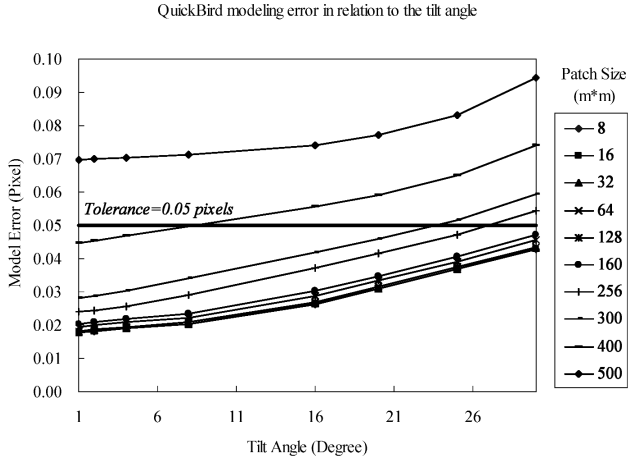

Figure 8. QuickBird modeling error in relation to the tilt angle.

TABLE 3. INFORMATION RELATED TO TEST IMAGES

	SPOT5	QuickBird
Location	Taipei, Taiwan	YingKe, Taiwan
Date	02 July 2002	26 May 2002
GSD (meters)	2.5 (Supermode)	0.6
Test Area (km × km)	60 × 60	16 × 18
Image Size (pixels × pixels)	24000 × 24000	28764 × 27552
Tilt Angle (degrees)	14.23	12.52
Number of GCPs	9	9
Number of ICPs	40	14
GCP and ICP Data Source	1:1000 Topographic Maps	
DTM	40 m Topographic Data Base of Taiwan	
Elevation Range (meters)	0 to 2100	0 to 700

160 m by 160 m. We spent 45 minutes to do the QuickBird orthorectification; for SPOT5, we spent 55 minutes.

We use SPOT5 data rather than QuickBird to do the Adaptive Patch Projection because its terrain variations and patch size are smaller. Also, when using quadtree to do the terrain analysis, the result is same as with an equal grid. The results are shown in Table 5. When using the Adaptive Patch Projection, orthorectification took only 28 minutes. Both the quality and computation time are satisfactory; 55 minutes was needed for equal grid patch projection, and more than 10 hours for the point-by-point method.

Summary

In this paper, (a) we propose a scheme for patch size optimization; the modeling error is less than 0.05 pixels; (b) the orbit adjustment accuracy is better than two pixels when there are nine ground control points; (c) the proposed "Adaptive Patch Projection" method can reduce the computation time needed for orthorectification; and (d) the orthorectifation result is better than two pixels, which is almost identical to the one tested in orbit modeling.

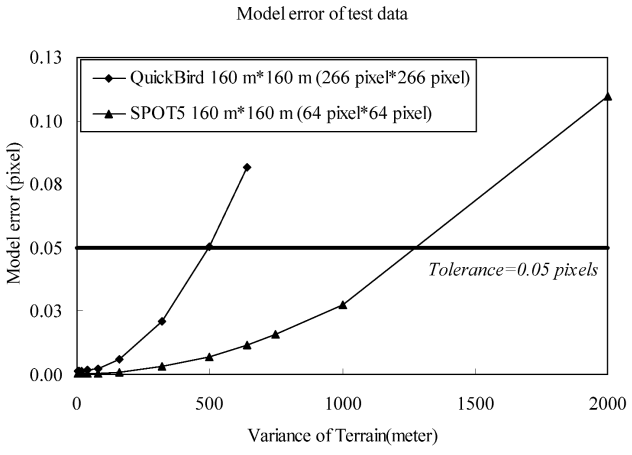

Figure 9. Modeling error of test data.

TABLE 4. ACCURACY ANALYSIS OF TEST DATA

			GCP		ICP	
	Unit: meters	GSD	RMSE E	RMSE N	RMSE E	RMSE N
Orbit Modeling	SPOT5	2.5	1.78	1.96	3.98	3.12
	QuickBird	0.6	0.55	0.48	0.71	0.87
Orthorectification	SPOT5	2.5	1.91	1.69	3.75	3.01
	QuickBird	0.6	0.60	0.51	0.83	0.90

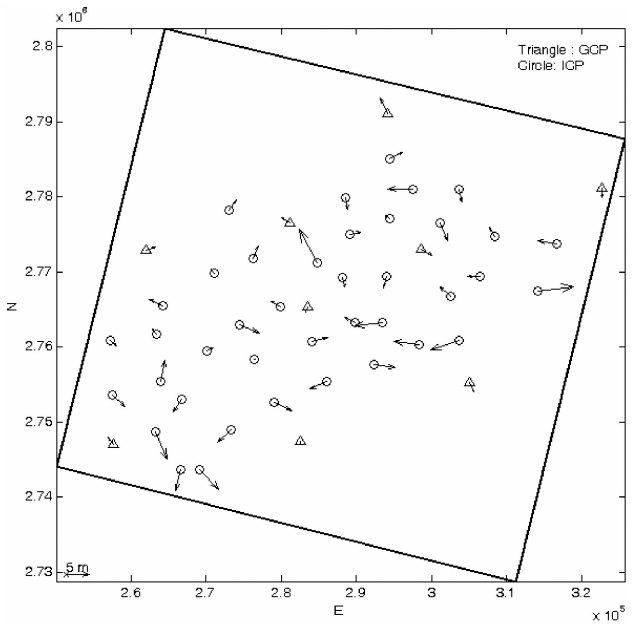

Figure 10. Error vectors for the generated SPOT5 orthophoto image.

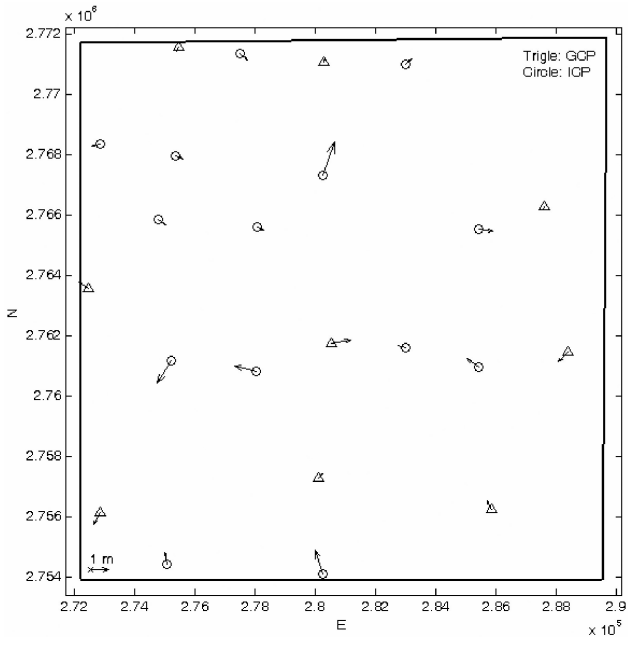

Figure 11. Error vectors for the generated QuickBird orthophoto image.

TABLE 5. COMPARISON OF COMPUTATION TIME FOR SPOT5

	Adaptive Patch Projection	Equal Grid Patch Projection	Point-by-Point
Computation Time (min.)	28	55	>10 hr
Terrain Variation (m)	0 to 2100	0 to 2100	0 to 2100
Patch size (m × m)	Max:1280 × 1280 Min:160 × 160	160 × 160	NULL
Terrain Allowance in a Patch (m)	500	NULL	NULL
Number of Patches	6,367	217,580	Number of Points: 5,760,000

Conclusions

In this study, we have proposed a procedure for the fast orthorectification of satellite images. The proposed method uses patch projection for orthorectification. Patch projection is seen to be a feasible way to improve the efficiency with respect to the point-by-point backprojection method. In order to control the modeling error of patch projection, modeling error analysis of the proposed method is also discussed. Data sets for SPOT5 and QuickBird data have been tested to validate the proposed method. The experimental results indicate that the proposed scheme can minimize the orthorectification computation time, while the modeling error is still insignificant.

Acknowledgments

This investigation was partially supported by the Remote Sensing Group of the Council of Agriculture under Project No. 92 AS 2.5.1-F2 (2). The authors would like to thank the Center for Space and Remote Sensing Research at the National Central University for providing the test data sets.

References

Chen, L.C., and L.H. Lee, 1993. Rigorous generation of digital orthophotos from SPOT images, *Photogrammetric Engineering & Remote Sensing*, 59(3):655–661.

Chen, L.C., and L.Y. Chang, 1998. Three dimensional positioning using SPOT stereo strips with sparse control, *Journal of Surveying Engineering*, ASCE, 124(2):63–72.

Chen, L.C., and T.A. Teo, 2002. Rigorous generation of digital orthophotos from EROS A high resolution satellite images, *International Archives of Photogrammetry & Remote Sensing*, 34(4):620–625.

Kim T., D. Shin, and Y.R. Lee, 2001. Development of robust algorithm for transformation of a 3D object point onto a 2D image point for linear pushbroom imagery, *Photogrammetric Engineering & Remote Sensing*, 67(4):449–452.

Konecny, G., P. Lohmann, H. Engel, and E. Kruck, 1987. Evaluation of SPOT imagery on analytical photogrammetric instruments, *Photogrammetric Engineering & Remote Sensing*, 53(9):1223–1230.

Mather, P.M., 1999. *Computer Processing of Remotely-sensed Images*, John Wiley & Sons, 292 pages.

Mikhail E.M., and F. Ackermann, 1982. *Observation and Least Squares*, University Press of America, New York, pp. 401.

Orun, A.B., and K. Natarajan, 1994. A modified bundle adjustment software for SPOT imagery and photography: tradeoff, *Photogrammetric Engineering & Remote Sensing*, 60(12): 1431–1437.

Toutin, T., 2003. Error tracking in Ikonos geometric processing using a 3D parametric model, *Photogrammetric Engineering & Remote Sensing*, 69(1):43–51.

Westin, T., 1990. Precision rectification of SPOT imagery, *Photogrammetric Engineering & Remote Sensing*, 56(2): 247–253.

(Received 01 June 2004; accepted 18 August 2004; revised 19 October 2004)